**Steel and Composite Structures**, *Vol. 32, No. 1 (2019) 127-139*
DOI: https://doi.org/10.12989/scs.2019.32.1.127


# Rehabilitation of corroded circular hollow sectional steel beam by CFRP patch

Mahdi Razavi Setvati [a] and Zahiraniza Mustaffa*

*Department of Civil and Environmental Engineering, Universiti Teknologi PETRONAS, 32610 Seri Iskandar, Perak, Malaysia*

(*Received December 9, 2018, Revised May 14, 2019, Accepted May 31, 2019*)

**Abstract.** Bridges, offshore oil platforms and other infrastructures usually require at some point in their service life rehabilitation for reasons such as aging and corrosion. This study explores the application of adhesively bonded CFRP patches in repair of corroded circular hollow sectional (CHS) steel beams. An experimental program involving three-point bending tests was conducted on intact, corroded, and repaired CHS beams. Meso-scale finite element (FE) models of the tested beams were developed and validated by the experimental results. A parametric study using the validated FE models was performed to examine the effects of different CFRP patch parameters, including patch dimensions, number of plies and stacking sequence, on efficiency of the repair system. Results indicates that the corrosion reduced elastic stiffness and flexural strength of the undamaged beam by 8.9 and 15.1%, respectively, and composite repair recovered 10.7 and 18.9% of those, respectively, compared to undamaged beam. These findings demonstrated the ability of CFRP patch repair to restore full bending capacity of the corroded CHS steel beam. The parametric study revealed that strength and stiffness of the repaired CHS beam can be enhanced by changing the fiber orientations of wet composite patch without increasing the quantity of repair materials.

**Keywords:** CFRP; patch; repair; circular hollow sectional steel beam; corrosion

## 1. Introduction

Damaged infrastructures are increasingly becoming a threat to public safety, economy and quality of life. According to the American Society of Civil Engineers (ASCE 2013), over 20% of the 607,380 bridges in the United States (US) are classified as structurally deficient or functionally obsolete, while the average age for all bridges is 42 years. Over 50% of the structurally deficient or functionally obsolete bridges in the US are made of steel (Deng and Lee 2009). According to the Federal Highway Administration (FHWA 2013), $20.5 billion are needed annually to eliminate deficiencies in the US's bridges over the next 15 years. A significant number of oil and gas platforms in the world are approaching or have exceeded their original design life, which was specified as typically 25 years. 127 fixed offshore platforms on the United Kingdom Continental Shelf (UKCS), approximately 50% of the total platforms, are beyond their original design life. It is evident that this proportion is continuously increasing with time, especially as the rates of platform decommissioning and new installations are fairly low (Stacey and Birkinshaw, 2008). Hollow sectional steel members have gained more widespread usage in bridges, airport terminal buildings, railway stations, industrial structures and oil platforms as load bearing in all directions and aesthetic appearance. Such existing steel structures are now facing the various level of damage due to corrosion, fatigue cracks, earthquake, and increasing live loads (Chen *et al*. 2015).

Conventional repair methods of damaged steel structures generally involve welding or bolting heavy steel plates to the existing structures (Gholami *et al*. 2016). Although such a repair approach has been utilized since 1934 (Tavakkolizadeh and Saadatmanesh 2003), major issues, such as a need to shut down production in offshore structures during welding and loss of a significant part of the cross sectional area due to bolting, are accompanied (Mahdi and Zahiraniza 2018). The implement of new materials and strengthening techniques become essential to resolve the issues (Sundarraja and Prabhu 2013). Previous studies have been established carbon fiber reinforced polymer (CFRP) as a promising alternative repair technique for damaged structures. The favorable mechanical properties of CFRP composites include high strength, corrosion resistance, and ease of application (Mohammed *et al*. 2017). It can be used externally to enhance the shear and flexural capacities of beams (Faris and Mehtab 2015). Despite the considerable amount of research and applications of FRP composites in reinforced concrete (RC) and masonry structures, efforts on using FRP materials to retrofit damaged steel structures have been relatively limited (Zhou *et al*. 2013). Previous studies on the CFRP repaired damaged steel beams have generally been concerned on I-sectioned beams with limited attention to hollow sectional steel beams (Chen *et al*. 2015). Amer *et al*. (2011) presented an experimental study into the behavior of CFRP repaired steel I-beams having various notch depths that simulate the level of initial damage. Galal *et al*. (2012) conducted an experimental program on 13 medium-scale I-sectioned steel beams to evaluate three repair schemes, namely: (1) adhesive-bonded CFRP plates; (2) adhesive-bonded CFRP sheets; and (3) unbonded CFRP sheets with

*Corresponding author, Associate Professor,
E-mail: zahiraniza@utp.edu.my
[a] Ph.D. Graduate, E-mail: Mahdi.UTP@gmail.com



ISSN: 1229-9367 (Print), 1598-6233 (Online)

ductile anchorage systems. Notched I-sectioned steel beams repaired by CFRP or a recently developed Carbon-fiber Hybrid-polymeric Matrix Composite (CHMC), which has been termed CarbonFlex, were studied experimentally and numerically by Zhou *et al*. (2013). Allan *et al*. (2016) experimentally investigated a pre-impregnated carbon fiber reinforced epoxy for repair of corroded and cracked I-sectioned steel beams. The results demonstrated the ability of carbon prepreg patch to repair crack and corrosion defects in I-sectioned steel beams, restoring them to their original strength and stiffness. Ephrem and Akbar (2012) experimentally investigated repair of damaged circular hollow sectional (CHS) steel beams using composite wrapping. However, the repair of an existing structure relies mostly on the available access for repair (Mohamed 2014) and in some cases it could be difficult to fully wrap the CHS beams by composite, especially when these beams used in the floor system or as a bridge's girder because the loads are applied on the top surface of the beams. In view of the reported literatures, it could be seen that there is a need to study repair of damaged CHS beams by composite materials. When composite patch/strip attaches to the bottom flange of an I-sectioned steel beam, it significantly improves the flexural capacities of the beam. Thus, following the same repair concept of steel I-sectioned beams, the CHS steel beams repaired from the underneath surface using the CFRP patch could be considered as an appropriate solution. Patch-type repairs, as opposed to fully encircled repairs, do not completely surround the damaged member, but rather only a specified area over the structural defect (Theisen and Keller 2016). The stiffness and strength of a finished composite part is dependent upon the orientations of its plies. This means that composite materials have advantages over metals in that we can design for stiffness and strength by tailoring the properties to suit the commodity, which could result in decreased cost. Therefore, there is a need for developing modeling approaches to predict the performance of steel beams repaired by wet lay-up CFRP with different fiber orientations. The objectives of the current study are: (1) to investigate the feasibility and effectiveness of CFRP patch for repair of corroded CHS steel beams; (2) to develop meso-scale FE models of the CFRP patch repaired CHS steel beam which can be used to evaluate the effects of various CFRP patch parameters, including fiber orientations, on the flexural behavior of the repaired beams.

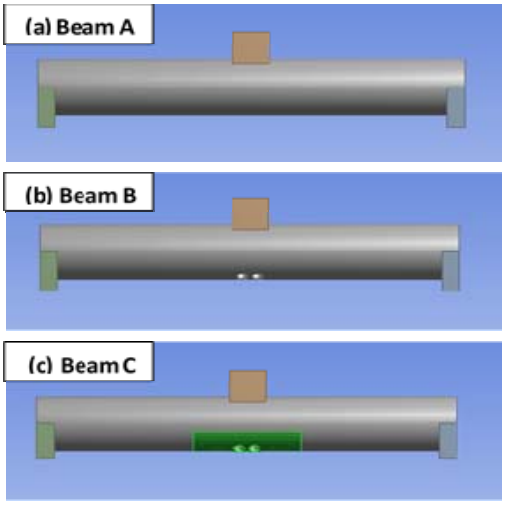


Fig. 1 CHS beams: (a) Intact beam (Beam A); (b) Corroded beam (Beam B); and (c) Repaired corroded beam

## 2. Experimental program

An experimental program was carried out to study the flexural performance of intact, corroded, and CFRP patch repaired CHS steel beams. Furthermore, experimental results were also used to validate the corresponding FE models. This section describes the properties of materials, details of experimental specimens, test setup and instrumentation.

### *2.1 Materials*

#### *2.1.1 Steel*

Three CHS steel beams were used in this study. Tensile tests were conducted to determine the mechanical properties of the steel beams. The results of the tensile tests show that the steel has Young's modulus, yield and tensile strength of 200 GPa, 264 MPa and 450 MPa, respectively.

#### *2.1.2 CFRP*

The carbon fiber fabric Sikawrap -231C and the epoxy impregnation resin Sikadur -330 were utilized as the repair materials. The Sikawrap and the Sikadur were chosen due to its wide structural applications (Jun and Marcus 2007). The Sikawrap -231C is a unidirectional carbon fiber fabric with high strength having a nominal thickness of 0.13 mm/ply and Sikadur -330 is a two-part thixotropic epoxy based impregnating resin/adhesive. The epoxy adhesive consisting of Part A (resin) and Part B (hardener). The Sikawrap -231C has strength of 4900 MPa, Young's modulus of 230 GPa, and maximum strain of 2.1% and Sikadur -330 has tensile strength of 30 MPa and Young's modulus of 4.5 GPa, as per the manufacturer's specifications.

### *2.2 Beam details*

Three CHS steel beams, including one undamaged control beam (Beam A), one corroded beam (Beam B), and one repaired corroded beam (Beam C), as shown in Fig. 1, were studied. The experimental samples have a length of 1170 mm, an external diameter of 168.3 mm and a wall thickness of 14.3 mm. Small-scale experimental samples, which have 1170 mm lengths, were considered to suit available experimental equipment. Cylindrical samples with high wall thickness of 168.3 mm were chosen to represent a structural element of a bridge or a jacket type offshore platform. The specimen preparation involved corrosion creation, surface preparation, and applying wet lay-up CFRP.

#### *2.2.1 Corrosion creation*

Different researchers have artificially created localized and/or distributed corrosion damage on steel structural elements by various techniques (Allan *et al*. 2016,

Mohamed 2014, Ephrem and Akbar 2012, Galal *et al*. 2012, Photiou *et al*. 2006, Abdullah *et al*. 2004). For example, Galal *et al*. (2012) drilled a few holes in tension flanges of I-sectioned steel beams to simulate deterioration in the flexural capacity of beams attributable to localized corrosion. In this study, six holes were drilled through the whole thickness of the cylinder at mid-span of two CHS beams, as shown in Fig. 2, to simulate structurally deficiency attributed to localized corrosion, following the same corrosion-simulation technique adopted by Galal *et al*. (2012). Details of created corrosion damage on the beams are given in Fig. 3. Localized corrosion damage was studied because firstly, in most cases, the damage due to corrosion is localized in the beam (Allan *et al*. 2016) and secondly, localized corrosion is considered to be more dangerous than uniform corrosion damage since it is more difficult to detect, predict and design against.

### 2.2.2 Surface preparation

Although proper surface preparation of steel substrate is an important step to achieve a good bond joint between the steel and CFRP (Mohamed 2014, Ephrem and Akbar 2012, and Akbar *et al*. 2010), specific requirements have not been developed yet (Amer *et al*., 2011). In this study the bottom surfaces of Beams C was roughened by an electric grinder with a sand paper wheel (roughness size #24) to enhance bond between the steel and composite material. It should be noted that same procedure was adopted by Yail and Garrett (2011) and Ahmed *et al*. (2017) for surface preparation. The surfaces of the samples were thoroughly cleaned with mechanical brush and acetone immediately prior to the application of composite repair. This was done to ensure that the surface was clean from any of the contaminants, such as dust and rust.

Fig. 2 Corrosion damage creation

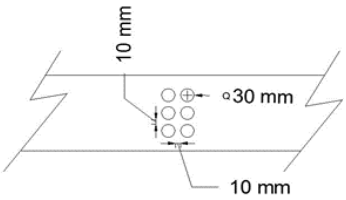


Fig. 3 Details of corrosion damage

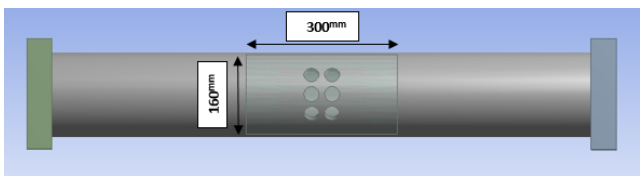


Fig. 4 Dimensions of CFRP patch

### 2.2.3 CFRP patch repair

Contrary to RC applications that have design standards and guidelines (ACI 2007), virtually no globally-accepted design guidelines are available for steel applications of CFRP composites (Amer 2014). Although analytical modeling based on sectional analysis is available for design of CFRP (wrap) strengthened undamaged CHS beam (Haedir *et al*. 2010, Haedir and Zhao 2012), currently there is no analytical modeling available for design of CFRP patch repaired damaged CHS steel beam. Therefore, in this study CFRP patch repairs were sized by trial-and-error method using finite element analysis (FEA) to be capable to restore the full flexural stiffness and strength of damaged beams. To keep the overall stiffness of the beam unchanged, stiffness of the CFRP patch, which is determined by the number of plies and orientations of its plies, is considered to be equal to stiffness of the corroded portion of the beam. One of corroded beams was repaired by a patch which was composed of 15 plies of identical 160×300 mm CFRP sheets, as shown in Fig. 4. It should be noted that a large number of composite layers is common in composite repair industry as Allan *et al*. (2016) used 15-ply composite, Karatzas *et al*. (2013) utilized 16-ply composite and Tsouvalis *et al*. (2008) used 18-ply composite for repair purpose. The carbon fiber sheets were applied underneath the corroded sample using a saturating epoxy as both a resin and adhesive in a wet lay-up (hand lay-up) system. The mixing ratio of Sikadur -330 part A to part B is 4:1 by weight, respectively. After the carbon fiber fabric was properly saturated with the adhesive, it was installed on the corroded beam manually while keeping the center of the patch with the center of the damage. First ply aligned with the longitudinal direction of the beam, while the second ply positioned at 90° to the longitudinal direction of sample, and this procedure was continued to the last ply. The CFRP repair was left to cure for two weeks in the laboratory prior to experimental testing.

### 2.3 Test setup and instrumentation

The specimens were subjected to three-point bending under static load conditions, as shown in Fig. 5. Such a testing scheme is particularly useful for studying the performance of damaged beams (Yail and Garrett 2011). One linear variable differential transformer (LVDT) was located at the mid span (immediately beneath the applied load) to measure the deflection of the sample. Three KYOWA, 2-mm-long, strain gauges were mounted on the surface of the CFRP patch to measure longitudinal strains of the composite repair. Fig. 6 shows the positions of the strain gauges on the experimental samples. The load, midspan deflection, and strains at different points were recorded with a data acquisition system interfacing with a PC.

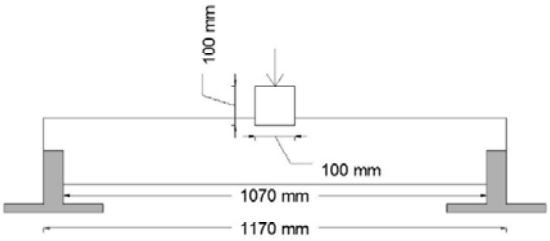


Fig. 5 Three-point bending test

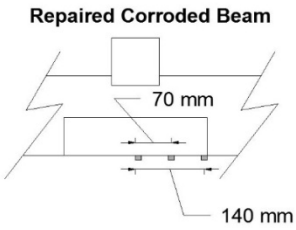


Fig. 6 Positions of strain gauges on repaired beam

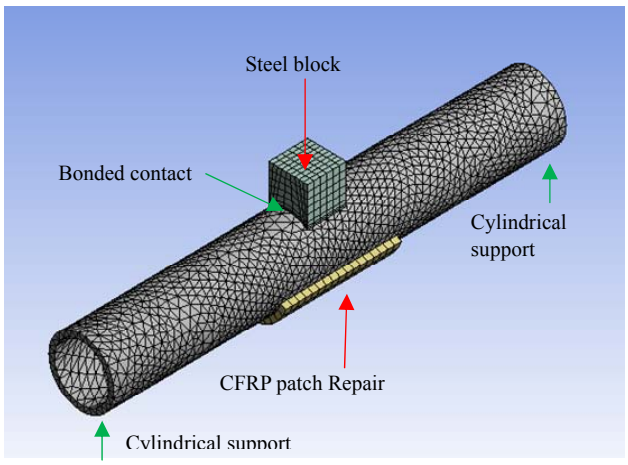


Fig. 7 Constructed FE model

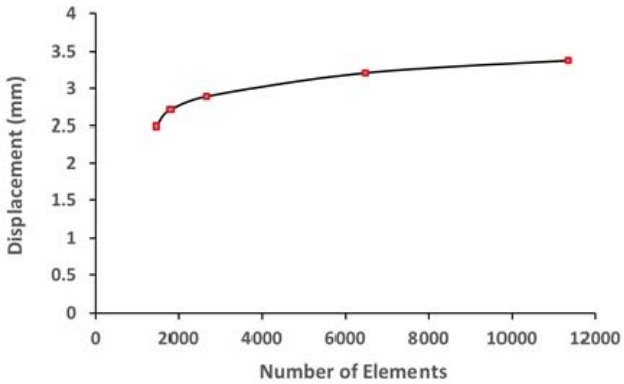


Fig. 8 Mesh convergence study

## 3. Proposed model

Numerical simulations have been used as complementary and cost-effective methods to experiments, as the latter could be time consuming and limited in its scope to cover extensive testing parameters (Wu *et al*. 2012). This section summarizes a modelling approach to predict the performance of damaged CHS steel beam repaired by CFRP patch when subjected to static loading. The FE modeling approach is unique because it takes into account fiber orientations and orthotropic behavior of wet lay-up CFRP. The FEA program ANSYS Workbench (Version 15) and ANSYS Composite PrepPost (ACP) Module, which is an add-on module to ANSYS, were utilized.

### *3.1 Mesh*

The geometrical models were meshed into elements, as shown in Fig. 7, using combination of the auto meshing and map meshing in order to achieve the best solution. It should be noted that Kambiz *et al*. (2012) implemented the same method (combination of auto meshing and map meshing) for meshing their finite element models and they achieved very accurate results. A relatively fine mesh was used based on the results of mesh convergence study, as shown in Fig. 8.

### *3.2 Element description*

The CHS steel beams were modeled with 3-D, higher order SOLID187 element. This element has a quadratic displacement behavior and is well suited for irregular meshes, such as those produced near damaged region. It should be noted that Ma *et al*. (2015) used SOLID187 for modelling tubular steel member and bolted-plate steel connections. SHELL181 elements were used to represent CFRP patch repair. SHELL181 can be used for layered applications for modeling composite shells or sandwich construction (ANSYS Inc. 2015). It should be noted that Pouria *et al*. (2015) employed SHELL181 for modelling composite layers (laminates). The interfacial behavior between composite and steel was model using CONTA174 and TARGE170 elements. CONTA174 is used to represent contact and sliding between 3-D "target" surfaces (TARGE170) and a deformable surface, defined by this element. It should be noted that similar elements and concept had been considered by Suzan (2018) for modelling interface between composite and steel.

### *3.3 Constitutive models*

#### *3.3.1 Steel*

While engineering stress strain curve can be used for small strain analysis, true stress strain must be used for

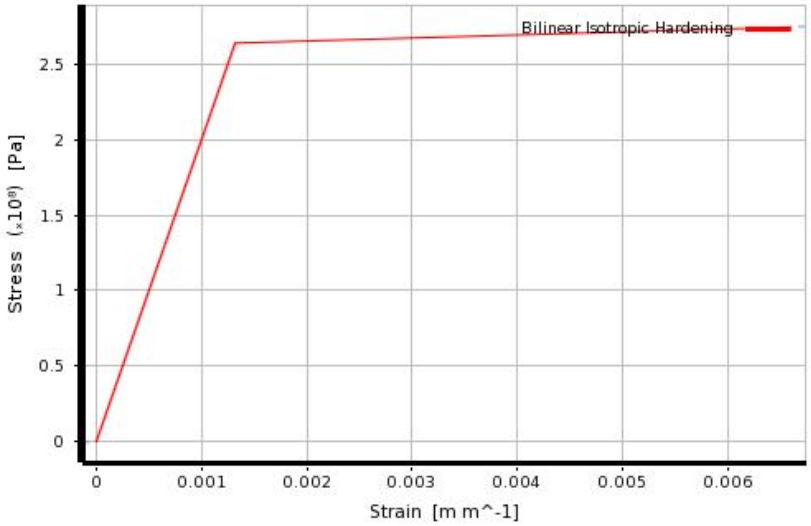


Fig. 9 Bi-linear isotropic hardening model of steel

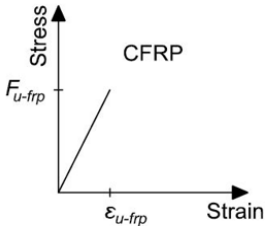


Fig. 10 Constitutive model of CFRP

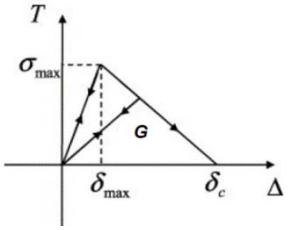


Fig. 11 The bilinear traction separation law (Karatzas *et al*. 2013)

plasticity, as they are more representative measures of the state of material (ANSYS Inc. 2014). It should be noted that Fernando *et al*. (2015, 2009), who studied CFRP-strengthened rectangular steel tubes, used true strain stress curve for their finite element analysis. The steel non-linearity (plasticity) was accounted for in the model by specifying a bi-linear isotropic hardening model, as shown in Fig. 9. The tangent modulus set as 2000 MPa in compliance with Eurocode 3 (2005). The bilinear isotropic hardening model was used in many numerical studies. For instance, Iftekharul and Sabrina (2015) used this modelling concept in the FEA of CFRP strengthened steel CHS column.

### *3.3.2 CFRP*

The CFRP laminate was treated as a linear (see Fig. 10) and orthotropic material. Number of layers, orientation of the fibers in each layer and thickness of each ply were defined in the ACP (Pre) Module.

### *3.3.3 Adhesive*

Several researchers, such as Burlović *et al*. (2016), Teng *et al*. (2015), Fernando *et al*. (2015), Kotsidis *et al*. (2014) and Anyfantis (2012), have implemented the Cohesive Zone Model (CZM) for modelling the adhesively bond between composite and metal and they have achieved very accurate results as in their related experimental results. The CZM is based on the concepts of stress and fracture mechanics, and can be fitted into the local or continuum approach (Da Silva and Campilho 2012). It is capable of simulating the damage initiation and growth (Karatzas *et al*. 2013). This approach introduces a failure mechanisms by gradually degrading the material elasticity between the surfaces. The material behavior at the interface is characterized by the stresses (normal and tangential) and separation distances (normal gap and tangential sliding) (CAE Associates 2012). The CZM is based on traction-separation constitutive law. Several shapes for the traction-separation law exist in the literature as follow: the bilinear, linear-parabolic, exponential and trapezoidal shapes. The bilinear law (Fig. 11) is well suited for the modeling of resins and non-ductile adhesives (Karatzas *et al*. 2013).

The material properties required for the cohesive law are:

(1) Maximum normal stress
(2) Maximum tangential stress
(3) Critical fracture energy for normal separation (mode I)
(4) Critical fracture energy for tangential slip (mode II)

In this study the CZM was used to model adhesive between composite and steel and CZM parameters were taken from Fernando *et al*. (2015), as summarized in Table 1. Fernando *et al*. (2015) calculated CZM parameters for the Sikadur-330 adhesive based on the approach which was proposed by Teng *et al*. (2015), Fernando (2010) and Campilho *et al*. (2008).

Table 1 Traction-separation parameters for Sikadur-330 adhesive

| Loading mode | Maximum stress (MPa) | Critical fracture energy (N/mm) |
|---|---|---|
| Mode I | 31.28 | 0.106 |
| Mode II | 28.15 | 7.056 |

### 3.4 Boundary conditions and loading

The cylindrical supports were assigned at two ends of the beams due to the curved surface of the CHS beam. The tangential movement was set into fixed while axial and radial movements were defined as free to keep the boundary conditions consistent with the experiments. The Bonded contact was defined between the top surface of the steel beam and the bottom surface of the block which transfers the applied load, as shown in Fig. 7. This Bonded contact fixes the surfaces to one another, so sliding or separation cannot occur. The load in the vertical direction at mid-span of the beam on a certain area corresponding to the load application region in the experimental tests was applied.

### 3.5 Validation and parametric study

The validation of FE approach was achieved in two steps. Firstly, the load-deflection curves of the three aforementioned beams obtained by computational simulation were compared with counterpart experimental results. Secondly, predicted strain distributions in the composite patch of Beam C were compared with corresponding strains measured by the strain gauges. There are several parameters that can affect the effectiveness of CFRP patch as a structural repair technique for damaged steel beams. The parametric study was performed by changing a single parameter while maintaining the remaining parameters constant.

## 4. Results and discussion

This section provides and discusses experimental and predicted results of the study, including load-deflection responses of three CHS steel beams, strain analysis of CFRP patch, stress analysis of steel beams, and effects of various composite patch parameters on the flexural performance of the CHS steel beam repaired by composite patching.

### 4.1 Load-displacement response

Figs. 12(a)-(c) show the midspan load-displacement responses of the predicted and experimental Beams A, B and C, respectively. These figures indicate that the predicted load-displacement response agreed well with that measured experimentally with average error of 8.9%. Experimental uncertainty, such as thickness of adhesive in a wet layup application, and assumptions in FEA, such as bilinear model of steel, could have contributed to the discrepancy.

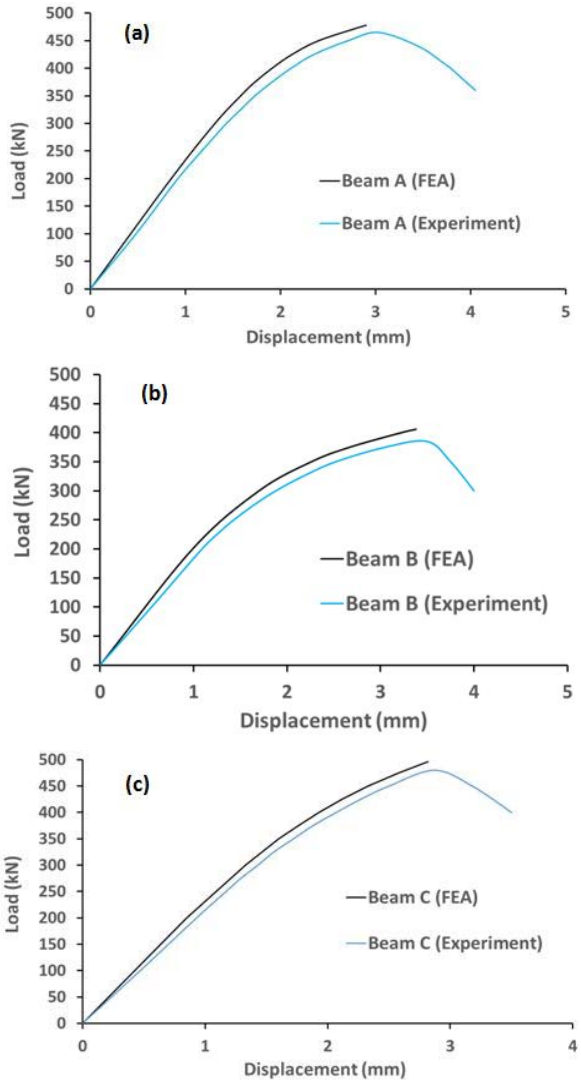


Fig. 12 Load-displacement response of (a) Beam A; (b) Beam Bl and (c) Beam C

The load-displacement curves became nonlinear, mainly because of the steel plasticity, following a linear elastic range. The Beams A and B failed by yielding of steel section, whereas the Beam C failed due to the rupture of CFRP patch, i.e., failure of CFRP in the transverse direction of patch by fiber breaking. This failure constitutes an intralaminar damage as the failure established inside a ply. The yielding of the beams was initiated exactly at the midspan and underneath of the beams, where the maximum strain occurred. Gradual load-softening was observed beyond the ultimate load of the experimental beams.

Fig. 13 compared load-displacement curves of computational Beams A, B and C. A summary of the predicted elastic stiffness and strength of the beams is given in Table 2. It can be observed that Beam C exhibited an increase in stiffness as well as ultimate strength, compared to the corroded beam (Beam B). The load-sharing mechanism between the steel and CFRP improved the flexural capacity of the repaired beams. The repair effect was more pronounced in the post-elastic region compared to the elastic region. This finding is consistent with observa-

Table 2 Predicted results of the beams

| Beam identification | Elastic stiffness (kN/mm) | Strength (kN) |
|---|---|---|
| Beam A | 224 | 478 |
| Beam B | 204 | 406 |
| Beam C | 228 | 496 |

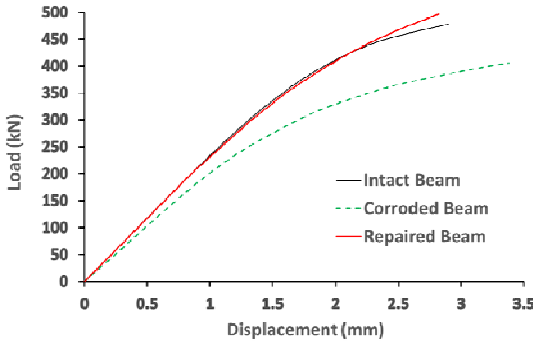


Fig. 13 Comparison of predicted results

tions from other studies by Ahmed *et al*. (2015, 2017), who conducted researches on the composite repaired concrete-filled steel tubular (CFST) beams. This finding can be explained by the fact that following yield, and the loss of stiffness of the steel, the contribution of the CFRP repair becomes greater. The elastic stiffness of corroded beam (Beam B) and repaired corroded beam (Beam C) are 204 and 228 kN/mm, respectively, which are 91.1 and 101.8% of that of undamaged beam (224 kN/mm). The flexural strength of corroded beam and repaired corroded beam are 406 and 496 kN, respectively, which are 84.9 and 103.8% of that of undamaged beam (478 kN). Therefore, the corrosion reduced elastic stiffness and flexural strength of the undamaged beam by 8.9 and 15.1%, respectively, and composite repair recovered 10.7 and 18.9% of those, respectively, compared to undamaged beam. These results demonstrated the ability of CFRP patch repair to restore full bending capacity of the corroded CHS steel beam.

### *4.2 Strain distributions in CFRP patch*

The longitudinal strain distributions in the composite patch of the repaired corroded beam (Beam C) at a load of 50% $P_u$ (typical service state) was graphed in Fig. 14. The computed strains agreed well with those measured experimentally. A symmetrical non-uniformly distribution shape was observed. The longitudinal strain at mid-span achieved the maximum value because the geometrical discontinuity at corroded region caused stress concentration at mid-span of the beam. The strain value significantly decreased away from mid-span to two terminations of the CFRP patch. It is worth nothing that Chen *et al*. (2015) reported that strains distribute non-uniformly in CFRP plate for nonprestressed specimen, and strains distribute uniformly in CFRP plate for prestressed specimen. Moreover, Chen *et al*. (2015) indicated that prestressed CFRP plate utilization efficiency is better than

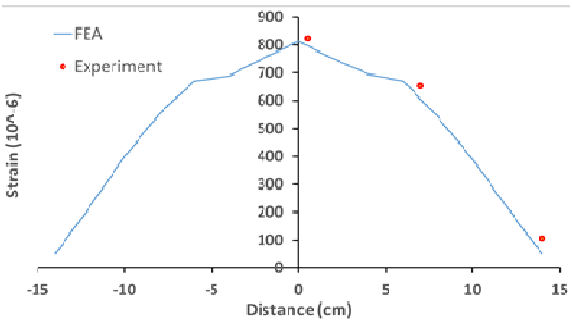


Fig. 14 Longitudinal strain distributions in CFRP patch of Beam C

nonprestressed one due to prevention of strain concentration at prestressed composite plate.

### *4.3 Stress distributions in CHS beam*

In comparison with experimental study, FEA is more comfortable and efficient for capturing stress distribution. The von Mises stress distributions in Beams A, B and C around the corroded area at a load of 157 kN (yield load of corroded beam), computed by the finite element analysis, are shown in Fig. 15. Maximum von Mises stress around the corroded area in Beam B (265.6 MPa) at a load of 157 kN was over two times greater than at same position in Beam A (117 MPa). Beam B started yielding and exhibiting local inelastic behavior at this load, while Beam A remained entirely elastic. These observations imply that damage in a CHS steel beam may cause significant stress concentration that could accelerate deterioration. It can be observed that composite repair reduced the maximum von Mises stress of the Beam B significantly by 23.3% from 265.3 to 203.6 MPa. Furthermore, CFRP Patch repair prevented the high stress concentration near corroded area and made stress distribution more uniform. This observation is attributed to the fact that composite patch repair effectively relieves some of the stress by reestablishing a continuous stress path for lower side of the beam.

### *4.4 Parametric study*

A parametric finite element study was performed to investigate the effects of various CFRP patch repair parameters (design variables) on the flexural behavior of the repaired CHS steel beams (response) and to determine the sensitivity of the flexural performance of repaired beams to the parameters.

#### *4.4.1 Effect of CFRP patch length*

Fig. 16 shows the effect of three CFRP patch lengths of 20, 30, and 40 cm on the flexural response of the repaired CHS beam. It can be seen that increasing the CFRP patch length increased the stiffness of the repaired beam. This was mainly because the longer patch increased the moment of inertia of the greater length of the repaired beam and, therefore, enhanced stiffness of the entire beam more. The stiffness enhancement was more pronounced in the post-elastic region in comparison with elastic region. This

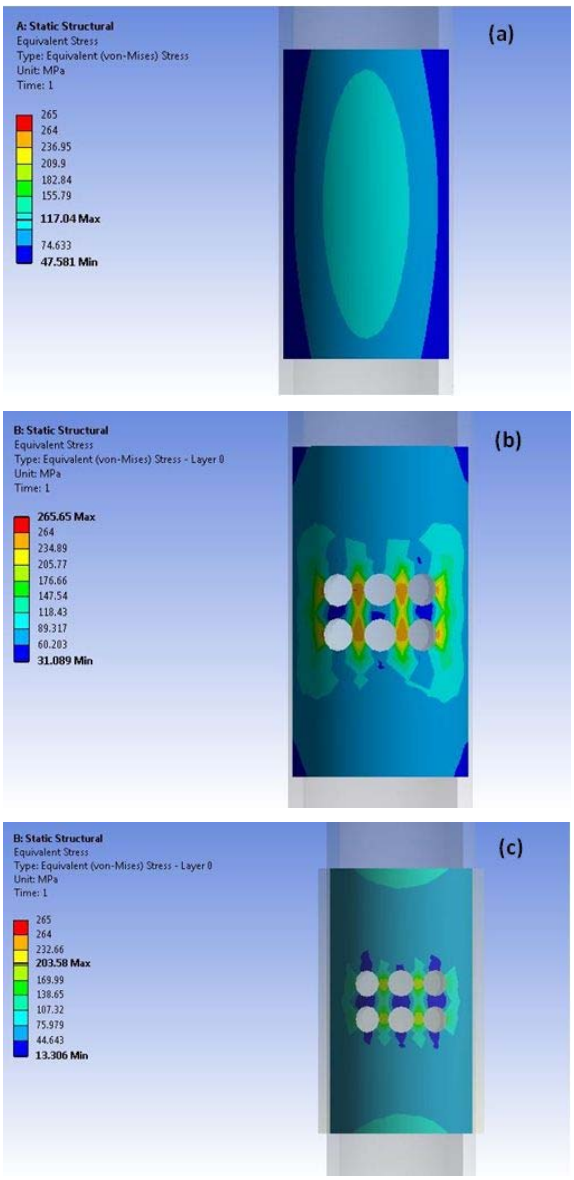


Fig. 15 Von Mises stress distributions in: (a) Beam A; (b) Beam B; and (c) Beam C

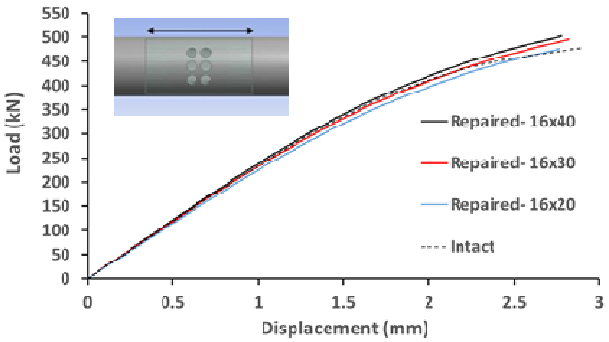


Fig. 16 Effect of CFRP patch length on the flexural performance of repaired beam

observation can be explained by the fact that following yield, and the loss of stiffness of the steel, the contribution of the CFRP patch repair becomes greater. The CFRP patch

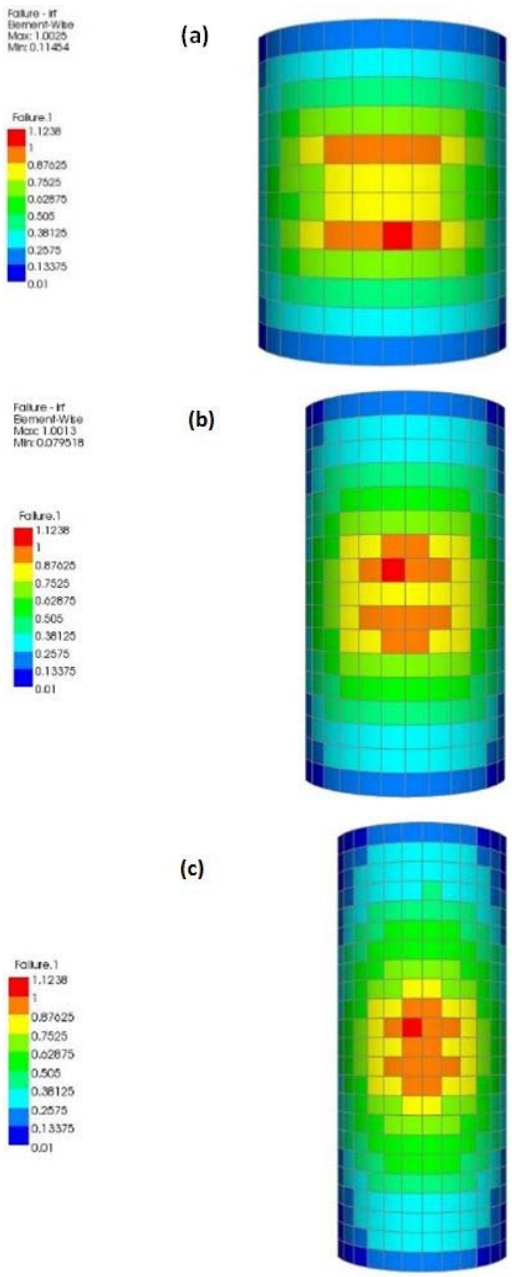


Fig. 17 Failure analysis of beams having CFRP patch lengths of (a) 20; (b) 30; and (c) 40 cm

repair length has slight effect on the strength of the repaired CHS beam. This is due to failure mechanism of the CFRP patch repair. The failure of CFRP patch based on various failure criteria of composite including maximum strain, maximum stress, Tsai-Wu, Tsai-Hill, Puck and Hashin was evaluated and visualized in ACP (Post). Figs. 17(a)-(c) show the results of failure analysis of repaired beams having patch length of 20, 30 and 40 cm, respectively. The critical failure criteria of the repaired beams are maximum strains in the longitudinal direction of the CHS beam. The critical region is the center of the patch because of strain concentration at this position. Lengthening the patch at its two ends in longitudinal direction of the beam had small effect on the center of the patch (critical region) and, thus, strength of the CHS beam.

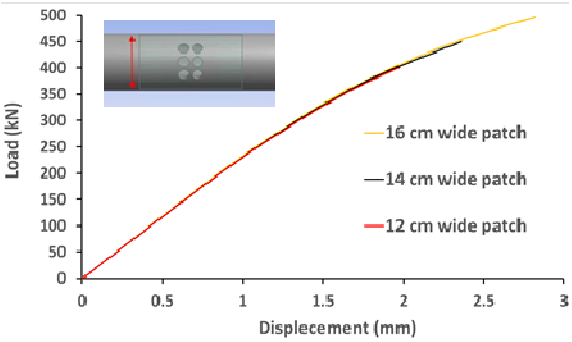


Fig. 18 Effect of CFRP patch width on the flexural performance of repaired beam

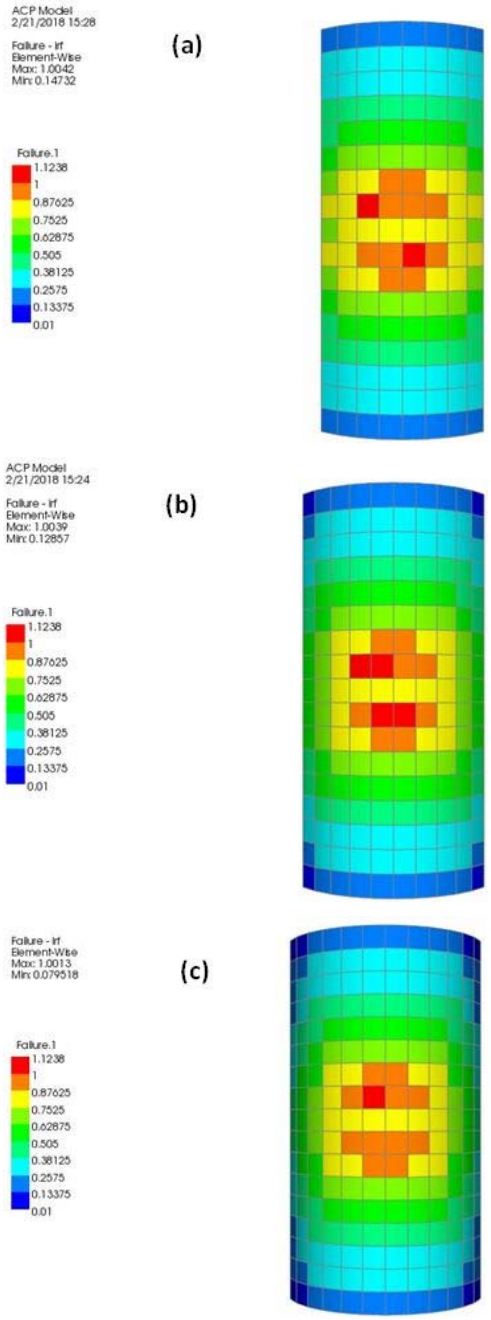


Fig. 19 Failure analysis of repaired beams having CFRP patch widths of (a) 12; (b) 14; and (c) 16 cm

### *4.4.2 Effect of CFRP patch width*

Flexural responses of repaired CHS beams having three CFRP patch widths of 12, 14 and 16 cm were depicted in Fig. 18. It can be seen that CFRP patch width had negligible effect on the stiffness of the repaired beam. This observation can be explained by the fact that increasing CFRP patch width from 12 to 16 cm resulted in adding composite repair near to position of neutral axis of the cross section and, therefore, it has negligible effect on the moment of inertia and flexural stiffness of the beam. Fig. 18 indicates that unlike the stiffness of the repaired beam, the strength recovery was affected significantly by the CFRP patch width. This is because of failure mechanism of the CFRP patch repair. Results of failure analysis of the repaired beams having three CFRP patch widths of 12, 14 and 16 cm are shown in Figs. 19(a)-(c), respectively. The critical failure criteria of the repaired beams are maximum strains in the longitudinal direction of the CHS beam. The critical region is the center of the patch, which is close to the corroded area of the steel beam, because of strain concentration at this position, which resulting from large deformation of the steel beam at this position. Widening the patch includes adding the repair material near the critical region of the CFRP patch repair. The greater amount of repair material at the critical region resulted in ability to carry more load and, therefore, prevented the early failure of composite and increased strength of the repaired beam.

### *4.4.3 Effect of number of CFRP plies*

Load-deflection curves of corroded beams having 10, 15, and 20-ply composite repairs were depicted in Fig. 20. It can be noticed that increasing the number of plies (CFRP thickness) enhanced the stiffness of the repaired beam. This is mainly because that thicker CFRP repair resulted in the greater moment of inertia of the cross section and, thus, stiffer beam. It was found that number of CFRP plies has substantial effect on the strength of the repaired beam. This is attributed to the failure mechanism of the repaired beam. Results of failure analysis of the repaired beams having 10, 15 and 20-ply CFRP patch are shown in Figs. 21(a)-(c), respectively. The critical failure criteria of the repaired beams are maximum strains in the longitudinal direction of the CHS beam. Increasing the thickness of the CFRP repair material strengthened it and as a consequence it can stand greater amount of longitudinal strain. This resulted in

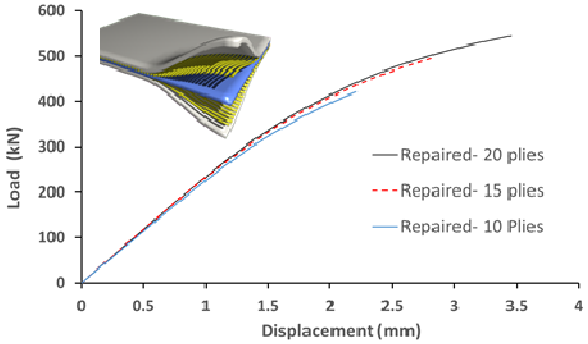


Fig. 20 Effect of number of CFRP plies on the flexural performance of repaired beam

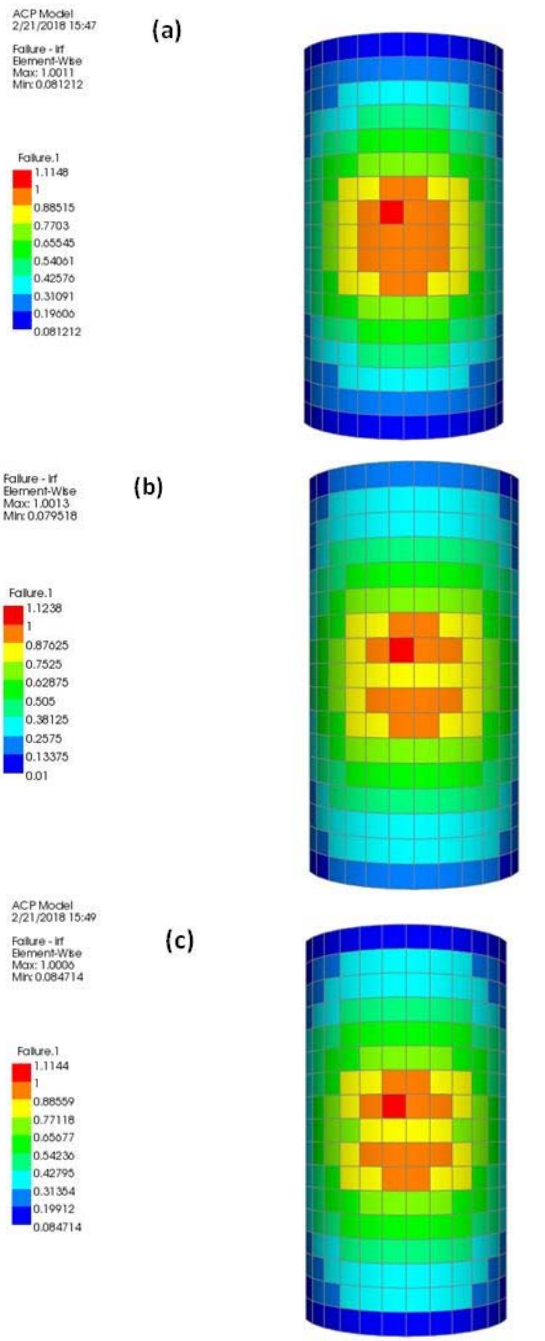


Fig. 21 Failure analysis of repaired beam having (a) 10-ply CFRP; (b) 15-ply CFRP; and (c) 20 ply-CFRP Patch

delaying the failure of composite repair and increasing strength of the repaired beam.

### *4.4.4 Effect of stacking sequence*

A summary of flexural behaviors of the repaired beams having three different stacking sequences, including [0°/+90°], [+45°/-45°/0°/+90°] and [+45°/-45°], is given in Fig. 22. These three stacking sequences were commonly observed in the composite applications (Allan *et al*. 2016, Gong *et al*. 2015, Harald *et al*. 2012, Papanikos *et al*. 2005). It can be observed that the repaired beam having stacking sequence of [0°/+90°] showed the highest stiffness

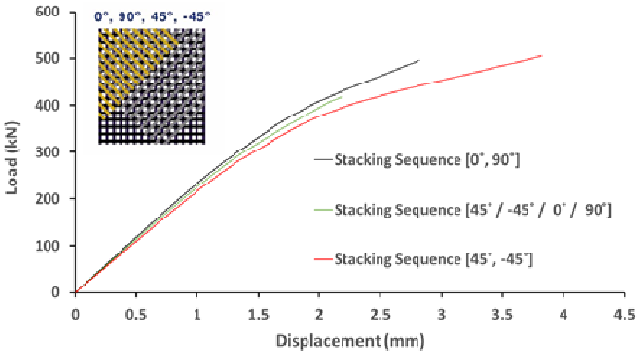


Fig. 22 Effect of stacking sequence on flexural behavior of repaired beam

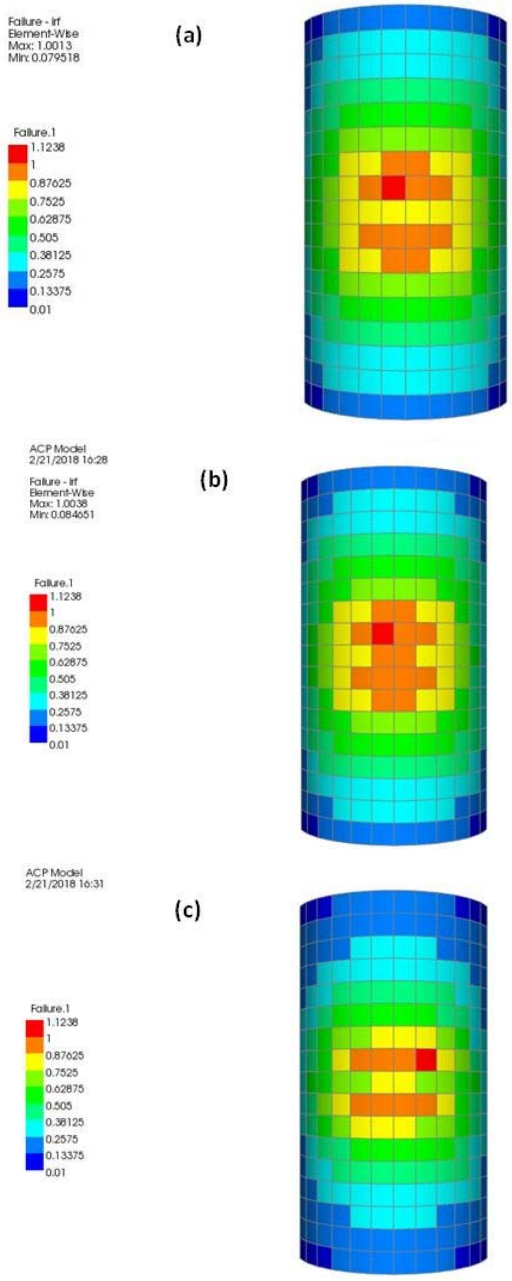


Fig. 23 Failure analysis of repaired beams having stacking sequences of (a) [0°/+90°]; (b) [+45°/-45°/0°/+90°] and (c) [+45°/-45°]

compared to the two other beams. This observation can be explained by the fact that this beam contains the maximum number of 0° layers, whose fiber orientation coincides to the longitudinal direction of the beam, and, therefore, its repair material is the stiffest in this direction, which resulted in the stiffest repaired beam. It can be noticed that repaired beam having stacking sequence of [+45°/-45°] exhibited the highest strength compared to the two other beams. This observation is attributed to the failure mechanism of the repaired beam. Results of failure analysis of the repaired beams having stacking sequences of [0°/+90°], [+45°/-45°/0°/+90°] and [+45°/-45°] are shown in Figs. 23(a)-(c), respectively. The critical failure criteria of the repaired beams are maximum strains in the longitudinal direction of the CHS beam. This beam contains no 90° layer (its fiber orientation is perpendicular to the longitudinal direction of the beam), which is the weakest fiber orientation for this particular beam configuration. This leads to preventing the early failure of repair material and, thus, the greatest strength of the beam. The effectiveness of the patch lay-ups with regard to stiffness and strength enhancement should not be the only criteria for their use as repairs. Other critical parameters, such as thermal expansion, must be also taken into account. For instance, although the quasi-isotropic [+45°/-45°/0°/+90°] did not show the most effective concerning the stiffness and strength improvement of the repaired beam, it is well known that it has smaller thermal expansion than the two other layups.

## 5. Conclusions

This paper has presented experimental and numerical investigations into the flexural behavior of CFRP patch repaired corroded CHS steel beams. Based on the measured and predicted results, the following is concluded:

- Results of this study demonstrated the ability of CFRP patch to recover 100% of lost flexural capacity of the corroded CHS steel beam and even to exceed its original capacity.
- The effect of composite patch repair technique on post-elastic stiffness was more pronounced compared to the elastic stiffness.
- The proposed FE modelling approach can be used for design of the wet lay-up CFRP patch repair and optimization of its fiber orientations.
- A non-uniformly strain distribution in CFRP patch indicted the presence of stress concentration at deficient area of the beam, reducing the efficiency of CFRP patch compared to prestressed CFRP plate, which has uniform strain distribution.
- Stress analysis of CHS steel beams showed that corrosion damage can increase the maximum von Mises stress of the damaged beam to over twice and CFRP patch repair reduced it significantly by 23.3%.
- Failure analysis of composite patch based on various failure criteria revealed that critical failure criteria is maximum strains in the longitudinal direction of the beam, which governs the failure of repaired beams.
- The parametric study using the validated FE model showed that increasing the CFRP laminates does not necessarily improve flexural stiffness and strength of repaired beams and proper CFRP laminate configuration is essential for maximum enhancement in bending behavior of beams.
- The sensitive parameters affecting the stiffness of CFRP patch repaired CHS steel beams are CFRP patch length, number of CFRP plies (CFRP thickness) and stacking sequence.
- The sensitive parameters affecting the strength of CFRP patch repaired CHS steel beams are CFRP patch width, number of CFRP plies and stacking sequence.
- The repaired beams having stacking sequences of [0°/+90°] and [+45°/-45°] exhibited the highest stiffness and the highest strength, respectively.

## Acknowledgments

The first author would like to thank for the graduate assistantship of the Universiti Teknologi PETRONAS (UTP) and acknowledge University Research Internal Fund (No. 153AA-B74) of UTP. Technical discussions with Prof. Dr. Nasir Shafiq of UTP, Dr. K.H. Leong of PETRONAS Research Sdn Bhd (PRSB), Engr. Biramarta Isnadi of PETRONAS Carigali Sdn Bhd (PCSB), and Dr. Zubair Imam Syed of Teesside University during this study project have been immensely useful and are gratefully acknowledged.

## References

Abdullah, H.A., Klaiber, F.W. and Wipf, T.J. (2004), "Repair of steel composite beams with carbon fiber-reinforced polymer plates", *J. Compos. Constr.*, **8**(2), 163-172. https://doi.org/10.1061/(ASCE)1090-0268(2004)8:2(163)

ACI (American Concrete Institute) (2007), Report on fiber reinforced polymer (FRP) reinforcement for concrete structures (ACI-440R-07); ACI Committee 440 (Fiber Reinforced Polymer Reinforcement), USA.

Ahmed, W.A.Z., Wan, H.W.B., Azrul, A.M. and Qahtan, A.H. (2015), "Finite element analysis of square CFST beam strengthened by CFRP composite material", *Thin-Wall. Struct.*, **96**, 348-358. https://doi.org/10.1016/j.tws.2015.08.019

Ahmed, W.A.Z., Wan, H.W.B., Azrul, A.M. and Salam, J.H. (2017), "Rehabilitation and strengthening of high-strength rectangular CFST beams using a partial wrapping scheme of CFRP sheets: Experimental and numerical study", *Thin-Wall. Struct.*, **114**, 80-91. https://doi.org/10.1016/j.tws.2017.01.028

Akbar, I., Oehlers, D.J. and Ali, M.M. (2010), "Derivation of the bond-slip characteristics for FRP plated steel members", *J. Constr. Steel Res.*, **66**, 1047-1056. https://doi.org/10.1016/j.jcsr.2010.03.003

Allan, M., Chamila, S., Warna, K., Lance, M.G. and Paul, F. (2016), "Pre-impregnated carbon fibre reinforced composite system for patch repair of steel I-beams", *J. Constr. Build. Mater.*, **105**, 365-376. https://doi.org/10.1016/j.conbuildmat.2015.12.172

Amer, H. (2014), "Crack-Dependent Response of Structural Steel Members Repaired with CFRP", Ph.D. Thesis; North Dakota State University, ND, USA.

Amer, H., Yail, J.K. and Siamak, Y. (2011), "CFRP Repair of Steel

Beams with Various Initial Crack Configurations", *J. Compos. Constr.*, **15**(6), 952-962. https://doi.org/10.1061/(ASCE)CC.1943-5614.0000223

Anyfantis, K.A. (2012), "Finite element predictions of composite-to-metal bonded joints with ductile adhesive materials", *J. Compos. Struct.*, **94**, 2632-2639. https://doi.org/10.1016/j.compstruct.2012.03.002

ANSYS Inc. (2014), ANSYS Composite PrepPost (ACP) Training. URL: https://support.ansys.com/AnsysCustomerPortal/en_us

ANSYS Inc. (2015), ANSYS Mechanical APDL Element Reference (V.15). URL: http://148.204.81.206/Ansys/150/ANSYS%20Mechanical%20APDL%20Element%20Reference.pdf

Blanco, N. (2012), "Failure criteria for composite materials", Presentation; Universitat de Girona, Spain.

Burlović, D., Milat, A., Balunović, M., Frank, D., Kotsidis, E.A., Kouloukouras, I.G. and Tsouvalis, N.G. (2016), "Finite element analysis of composite-to-steel type of joint for marine industry", *J. Weld. World*, **60**(5), 859-867. https://doi.org/10.1007/s40194-016-0343-7

CAE Associates (2012), ANSYS Cohesive Zone Modeling; Website of CAE Associates. URL: https://caeai.com/ansys-training

Campilho, R.D.S.G., Moura, M.F.S.F. and Domingues, J.J.M.S. (2008), "Using a cohesive damage model to predict the tensile behaviour of CFRP single-strap repairs", *Int. J. Solids Struct.*, **45**(5), 1497-1512. https://doi.org/10.1016/j.ijsolstr.2007.10.003

Chen, T., Qi, M., Gu, X.L. and Yu, Q.Q. (2015), "Flexural strength of carbon fiber reinforced polymer repaired cracked rectangular hollow section steel beams", *J. Polym. Sci.* http://dx.doi.org/10.1155/2015/204861

Da Silva, L.F. and Campilho, R.D. (2012), *Advances in Numerical Modelling of Adhesive Joints*, Springer.

Deng, J. and Lee, M.M.K. (2009), "Adhesive bonding in steel beams strengthened with CFRP", *J. Struct. Build.*, **162**, 241-249. https://doi.org/10.1680/stbu.2009.162.4.241

Ephrem, A. and Akbar, I. (2012), "The flexural behaviour of tubular steel member strengthened with CFRP", *Proceedings of 8th Asia Pacific Structural Engineering and Construction Conference and 1st International Conference for Civil Engineering Research*, Surabaya, Indonesia.

Eurocode 3 (2005), Design of Steel Structures—Parts 1-8: Design of Joints (BSEN 1993-1-8:2005), Standards Policy and Strategy Committee.

Faris, A.U. and Mehtab, A. (2015), "Steel-CFRP composite and their shear response as vertical stirrup in beams", *Steel Compos. Struct.*, *Int. J.*, **18**(5), 1145-1160. http://dx.doi.org/10.12989/scs.2015.18.5.1145

Fernando, D. (2010), "Bond Behaviour and Debonding Failures in CFRP-strengthened Steel Structures", Ph.D. Thesis; Department of Civil and Structural Engineering, Hong Kong Polytechnic University, Hong Kong, China.

Fernando, D., Yu, T., Teng, J.G., and Zhao, X.L. (2009), "CFRP strengthening of rectangular steel tubes subjected to end bearing loads: Effect of adhesive properties and finite element modelling", *Thin-Wall. Struct.*, **47**, 1020-1028. https://doi.org/10.1016/j.tws.2008.10.008

Fernando, D., Yu, T. and Teng, J.G. (2015), "Behavior and modeling of CFRP-strengthened rectangular steel tubes subjected to a transverse end bearing load", *Int. J. Struct. Stabil. Dyn.*, **15**(8). https://doi.org/10.1142/S0219455415400313

Galal, K., Seif, E.H.M. and Tirca, L. (2012), "Flexural Performance of Steel Girders Retrofitted Using CFRP Materials", *J. Compos. Constr.*, **16**(3), 265-276. https://doi.org/10.1061/(ASCE)CC.1943-5614.0000264

Gholami, M., Mohd S.A.R., Marsono, A.K., Tahir, M.M. and Faridmehr, I. (2016), "Performance of steel beams strengthened with pultruded CFRP plate under various exposures", *Steel Compos. Struct., Int. J.*, **20**(5), 999-1022. http://dx.doi.org/10.12989/scs.2016.20.5.999

Gong, X.J., Cheng, P., Aivazzadeh, S. and Xiao, X. (2015), "Design and optimization of bonded patch repairs of laminated composite structures", *J. Compos. Struct.*, **123**, 292-300. https://doi.org/10.1016/j.compstruct.2014.12.048

Haedir, J. and Zhao, X.L. (2012), "Design of CFRP-strengthened steel CHS tubular beams", *J. Constr. Steel Res.*, **72**, 203-218.

Haedir, J., Zhao, X.L., Bambach, M.R. and Grzebieta, R.H. (2010), "Analysis of CFRP externally-reinforced steel CHS tubular beams", *J. Compos. Struct.*, **92**, 2992-3001.

Harald, O., Dag, M.G., Jan, R.W. and Geir, O.G. (2012), "Predicting failure of bonded patches using a fracture mechanics approach", *Int. J. Adhes. Adhes.*, **37**, 102-111.

Hui-Huan, M., Ali, M.I., Feng, F. and Guy, O.A. (2015), "An experimental and numerical study of a semi-rigid bolted-plate connections (BPC)", *Thin-Wall. Struct.*, **88**, 82-89. https://doi.org/10.1016/j.tws.2014.11.011

Iftekharul, A.M. and Sabrina, F. (2015), "Numerical studies on CFRP strengthened steel columns under transverse impact", *J. Compos. Struct.*, **120**, 428-441. https://doi.org/10.1016/j.compstruct.2014.10.022

Jun, D. and Marcus, M.K.L. (2007), "Behaviour under static loading of metallic beams reinforced with a bonded CFRP plate", *J. Compos. Struct.*, **78**, 232-242. https://doi.org/10.1016/j.compstruct.2005.09.004

Kambiz, N., Ramli, S. and Mohd, Z.J. (2012), "Failure analysis and structural behaviour of CFRP strengthened steel I-beams", *J. Constr. Build. Mater.*, **30**, 1-9. https://doi.org/10.1016/j.conbuildmat.2011.11.009

Karatzas, V., Kotsidis, E. and Tsouvalis, N. (2013), "An Experimental and Numerical Study of Corroded Steel Plates Repaired with Composite Patches", *Proceedings of the 4th International Conference on Marine Structures*, *MARSTRUCT 2013*, Espoo, Finland.

Kotsidis, E.A., Kouloukouras, I.G. and Tsouvalis, N.G. (2014), "Finite element parametric study of a composite-to-steel-joint", In: *Maritime Technology and Engineering*, Taylor & Francis Group, London, UK, pp. 627-635.

Ma, H.H., Issa, A.M., Fan, F. and Adeoti, G.O. (2015), "An experimental and numerical study of a semi-rigid bolted-plate connections (BPC)", *Thin-Wall. Struct.*, **88**, 82-89. https://doi.org/10.1016/j.tws.2014.11.011

Mahdi, R.S. and Zahiraniza, M. (2018), "Rehabilitation of notched circular hollow sectional steel beam using CFRP patch", *Steel Compos. Struct., Int. J.*, **26**(2), 151-161. https://doi.org/10.12989/scs.2018.26.2.151

Mohamed, E. (2014), "CFRP strengthening and rehabilitation of degraded steel welded RHS beams under combined bending and bearing", *Thin-Wall. Struct.*, **77**, 86-108. https://doi.org/10.1016/j.tws.2013.12.002

Mohammed, H.S., Essam, G.S. and Ahmed, F.H. (2017), "Numerical study on the rotation capacity of CFRP strengthened cold formed steel beams", *Steel Compos. Struct., Int. J.*, **23**(4), 385-397. https://doi.org/10.12989/scs.2017.23.4.385

Papanikos, P., Tserpes, K.I., Labeas, G. and Pantelakis, S.P. (2005), "Progressive damage modelling of bonded composite repairs", *J. Theor. Appl. Fract. Mech.*, **43**, 189-198. https://doi.org/10.1016/j.tafmec.2005.01.004

Photiou, N.K., Hollaway, L.C. and Chryssanthopoulos, M.K. (2006), "Strengthening of an artificially degraded steel beam utilising a carbon/glass composite system", *J. Constr. Build. Mater.*, **20**, 11-21. https://doi.org/10.1533/9781845690649.3.274

Pouria, T.A., Saeid, S., Vaclav, K. and Habiba, B. (2015), "Investigating stress shielding spanned by biomimetic polymer-composite vs. metallic hip stem: A computational study using

mechano-biochemical model", *J. Mech. Behav. Biomed. Mater.*, **41**, 56-67. https://doi.org/10.1016/j.jmbbm.2014.09.019

Stacey, A. and Birkinshaw, M. (2008), "Life Extension Issues for Aging Offshore Installations", *Proceedings of 27th International Conference on Offshore Mechanics and Arctic Engineering* (*OMAE 2008*), Estoril, Portugal.

Sundarraja, M.C. and Prabhu, G.G. (2013), "Flexural behaviour of CFST members strengthened using CFRP Composites", *Steel Compos. Struct., Int. J.*, **15**(6), 623-643. https://doi.org/10.12989/scs.2013.15.6.623

Suzan, A.A.M. (2018), "Experimental and FE investigation of repairing deficient square CFST beams using FRP", *Steel Compos. Struct., Int. J.*, **29**(2), 187-200. https://doi.org/10.12989/scs.2018.29.2.187

Tavakkolizadeh, M. and Saadatmanesh, H. (2003), "Repair of damaged steel-concrete composite girders using carbon fiber-reinforced polymer sheets", *J. Compos. Constr.*, **7**(4), 311-322. https://doi.org/10.1061/(ASCE)1090-0268(2003)7:4(311)

Teng, J.G., Fernando, D. and Yu, T. (2015), "Finite element modelling of debonding failures in steel beams flexurally strengthened with CFRP laminates", *J. Eng. Struct.*, **86**, 213-224. https://doi.org/10.1016/j.engstruct.2015.01.003

Theisen, S.A. and Keller, M.W. (2016), "Comparison of Patch and Fully Encircled Bonded Composite Repair", *Mech. Compos. Multi-funct. Mater.*, **7**, 101-106. https://doi.org/10.1007/978-3-319-41766-0_11

Tsouvalis, N.G., Mirisiotis, L.S. and Tsiourva, T.E. (2008), "Experimental Investigation of Composite Patch Reinforced Corroded Steel Plates in Static Loading", *Proceedings of the 13th European Conference on Composite Materials* (*ECCM-13*) Stockholm, Sweden.

Wu, C., Zhao, X., Duan, W.H. and Al-Mahaidi, R. (2012), "Bond characteristics between ultrahigh modulus CFRP laminates and steel", *Thin-Wall. Struct.*, **51**, 147-157. https://doi.org/10.1016/j.tws.2011.10.010

Yail, J.K. and Garrett, B. (2011), "Interaction between CFRP-repair and initial damage of wide-flange steel beams subjected to three-point bending", *J. Compos. Struct.*, **93**(8), 1986-1996. https://doi.org/10.1016/j.compstruct.2011.02.024

Yail, J.K. and Kent, A.H. (2011), "Fatigue behavior of damaged steel beams repaired with CFRP strips", *J. Eng. Struct.res*, **33**, 1491-1502. https://doi.org/10.1016/j.engstruct.2011.01.019

Yail, J.K. and Kent, A.H. (2012), "Predictive response of notched steel beams repaired with CFRP strips including bond-slip behavior", *J. Struct. Stabil. Dyn.*, **12**(1), 1-21. https://doi.org/10.1142/S0219455412004628

Zhou, H., Attard, T.L., Wang, Y., Wang, J.A. and Ren, F. (2013), "Rehabilitation of notch damaged steel beams using a carbon fiber reinforced hybrid polymeric-matrix composite", *J. Compos. Struct.*, **106**, 690-702. https://doi.org/10.1016/j.compstruct.2013.07.001

*CC*